Chapter 7

Characterization of YBCO/Ag/YBCO joints: superconducting properties

7.1 Methodology for the determination of the critical current density

The critical current density in type II superconductors is a fundamental parameter, which is not only of interest to technical applications. It also offers a wide field of basic physics, related to the collective interaction of the vortex line lattice with structural and thermal disorder. There are several methods to determine j_c. In general, one has to distinguish between the global critical current density $\overline{j_c}$, which is measured by transport or magnetization measurements, and represents an average over the whole sample, and the local critical current density j_c. This can be determined by space-resolved measurements like Hall probes [29,30,90,91], or magneto-optics [92,93,94]. The difference between both critical current densities is caused by inhomogeneities in the superconductor, like macroscopic defects, weak links and by the local-magnetic field dependence of $j_c(B)$.

The methodology used in this work for the determination of the local critical current density is based on the Bean model. According to this model the spatial gradient of H or j_c is constant inside the sample. In a real case, the crit-

ical current density is dependent on B, and therefore j_c is not constant in the superconductor. However, it has been shown that the Bean model gives a good approximation for understanding the magnetic behavior of type II superconductors.

Figure 7.1a shows the current density stream lines in the critical state for a type II superconductor of square shape. The critical currents flow parallel to the sample edge and the current stream lines have sharp bends. The critical current distribution shows a pattern of critical current density domains of uniform parallel current flow which are separated by critical current density domain boundaries. In the framework of the Bean model, the bending of the critical current density is discontinuous and the size of the critical current density domain boundaries becomes infinitesimal small. In this case they form discontinuity lines (d lines) which divide the superconductor into domains with uniform parallel current flow. One distinguishes two types of d lines [95]: at d^+ lines the orientation of j_c changes discontinuously but the magnitude of j_c remains the same. On the contrary, at d^- lines the magnitude of j_c changes, e.g., at the specimen surface or at inner boundaries where regions at different j_c meet.

In isotropic rectangular superconductors, the d^+ lines run along the bisection lines starting from the sample corners and on a section of the middle line parallel to the longer side as shown in figure 7.1b.

Characteristic features of d^- and d^+ lines are the following:

1. d^- lines can be observed at internal and external boundaries of the sample, while d^+ lines separate the superconductor into regions with homogeneous current flow and are determined by the shape of the sample as it is seen in figure 7.1.

2. flux lines cannot cross the d^+ lines since during increase or decrease of the applied magnetic field the flux lines move towards or away from the d^+ lines, respectively. In contrast, d^- lines can be crossed by flux, e.g. when flux lines penetrate from the surface.

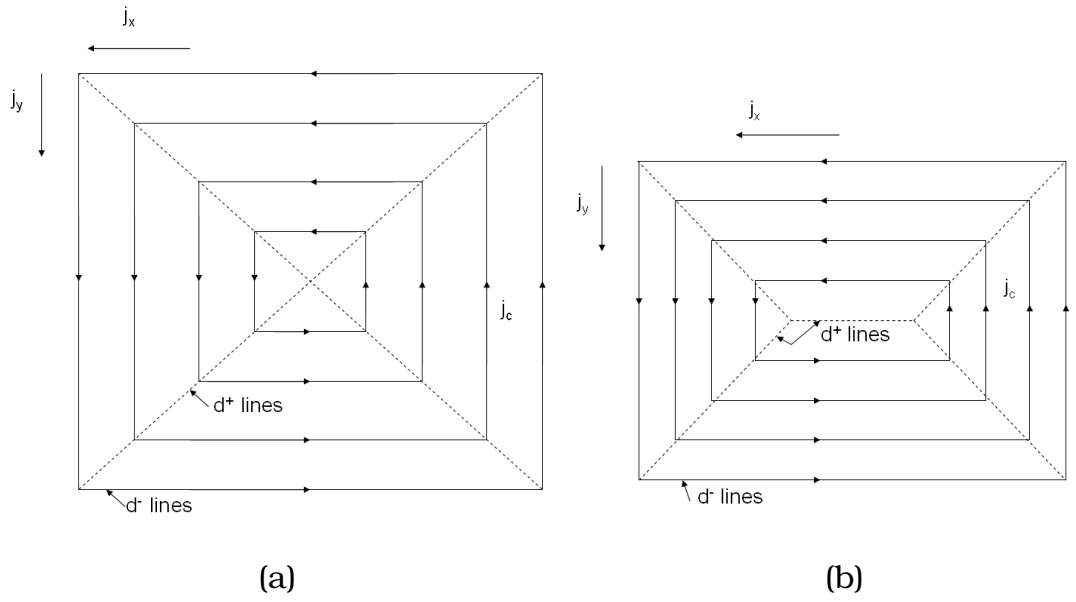

Figure 7.1: Critical current density distribution for a fully-penetrated magnetic flux single domain in the Bean model for a: a) square shaped superconductor; b) rectangle geometry. The d lines are indicated in the figure.

The use of this model has been extended for a bicrystal case. The flux penetration into a bicrystalline superconductor starts in the region with lower critical current density which is the grain boundary. In this case two critical current densities can be distinguished: a current which flows inside the grain (J_c^{grain}) and a current which flows across the grain boundary (J_c^{gb}).

In the framework of Bean critical state model with a constant intragrain critical current density (J_c^{grain}) and constant intergrain critical current density (J_c^{gb}), a model for the critical current density pattern near the grain boundary can be given [95]. Figure 7.2 shows a schematic representation of the critical current density pattern near the grain boundary for the ratio J_c^{gb}/J_c^{grain}=0.5. Typically there is a three fold bending of current stream lines around the grain boundary. Outside the grain boundary, the line on which the magnetization currents sharply change direction (d^+ line) and the grain boundary line form an angle α. This angle can be determined as follows:

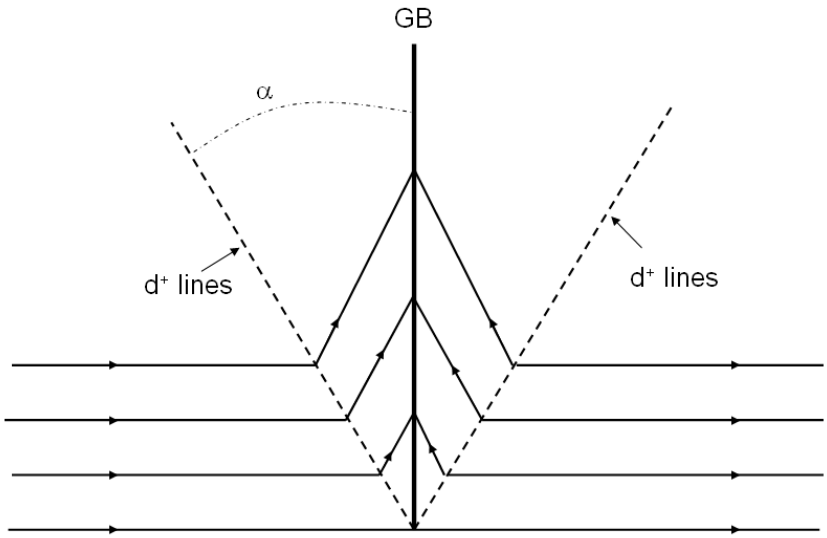

Figure 7.2: Sketch of the critical current density distribution at a grain boundary with a ratio J_c^{gb}/J_c^{grain}=0.5 assuming Bean´s model. α is the angle formed by the d^+ lines with the grain boundary and is determined by equation 7.1.

$$\alpha = \frac{1}{2} arcos(\frac{J_c^{gb}}{J_c^{grain}}) \tag{7.1}$$

According to this equation, α depends on the ratio J_c^{gb}/J_c^{grain} and this dependence is shown in figure 7.3. As can be seen in the figure it is not a linear dependence. For J_c^{gb}=J_c^{grain} and α=0 the pattern of the stream lines is similar to the pattern predicted by the model indicated in figures 7.1(a-b). For J_c^{gb}=0, equation 7.1 gives the well-known result α=45° of the isotropic Bean model for two rectangular samples.

Figure 7.4 shows the current stream lines determined according to this pattern for two samples with rectangular shape with J_c^{gb}/J_c^{grain}=0.5 (figure 7.4a) and J_c^{gb}/J_c^{grain}=0.25 (figure 7.4b). For the first case the angle α=30° and for the later case α=38°. Note that the current penetration through the grain boundary (blue lines) is faster than the penetration inside the grains (red lines) since the critical current density of the grain boundary is lower. When the stream line

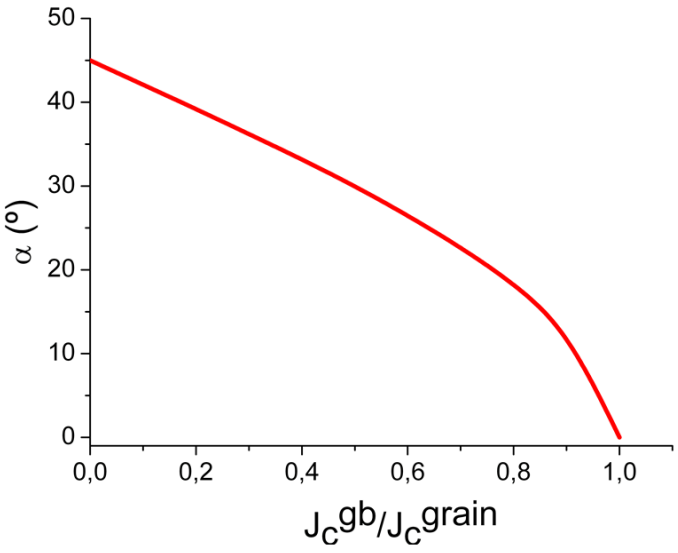

Figure 7.3: Dependence of the angle α with the ration J_c^{gb}/J_c^{grain}.

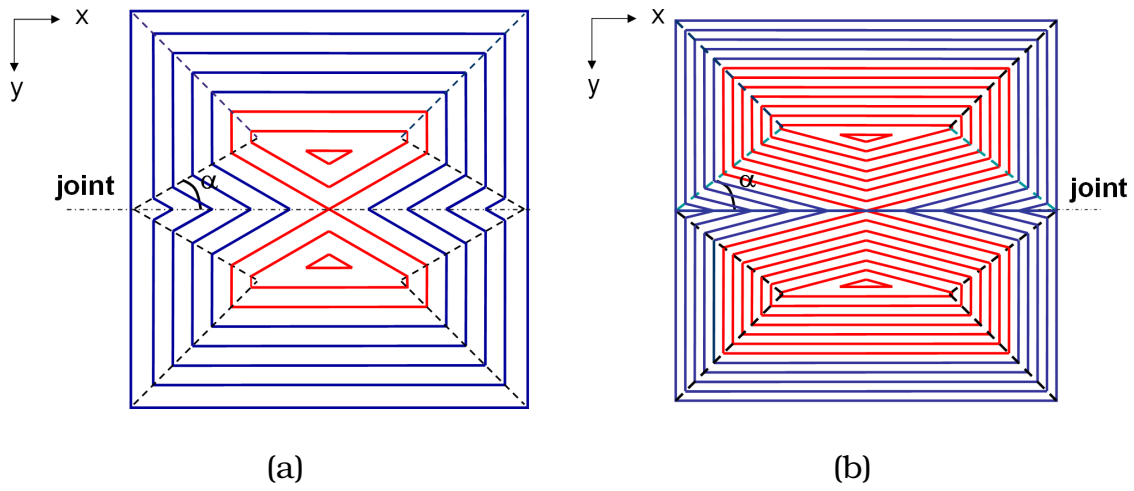

Figure 7.4: a) Current distribution calculated for two rectangular bicrystals with: a) J_c^{gb}/J_c^{grain}=0.5; b) J_c^{gb}/J_c^{grain}=0.25. The angle α is indicated in the figures. The blue lines indicate intergrain critical current and the red lines the intragranular critical current loops.

critical current density reaches the center of the sample, closed critical current density loops are formed inside the grains (red lines). From these figures, it can be observed that decreasing the ratio J_c^{gb}/J_c^{grain}, the penetration of current lines through the grain boundary occurs faster and, thus, the magnetic grain size is larger. Therefore, two kind of induced current loops can be distinguished : those extending through the whole sample indicated by blue lines in the figures and those that cannot extend more than a grain (red lines in the figures). The formation of unconnected current loops depends on both parameters: the size of the bicrystal and the ratio J_c^{gb}/J_c^{grain}.

As it was mentioned before, according to the Bean model the critical current density is constant all over the sample, thus J_c =J_{cx} =J_{cy}. In the rhombus area represented in figures 7.5 (light pink being positive component, whereas dark pink being negative component), there exist both, x and y components of the critical current density. The x component can be determined from the trapezium areas indicated by blue color and the y component from triangle areas indicated by granatum color in the figure. The x component of J_c, J_{cx}, is associated of the current flowing parallel to the joint whereas the y component, J_{cy} is associated of the current crossing the weld. For instance, the y component J_{cy} is the only one which could give us directly the critical current density of the joint. On the other hand, the critical current density of the YBCO grains, can be determined from both components of J_c, x and y. For the simplicity of the method proposed by us to determine simultaneously both critical current densities, of the YBCO material (J_c^{grain}) and of the joint (J_c^{gb}), we have considered only the y component of J_c.

If we consider only the y component of critical current density J_{cy}, the current distribution pattern should present the profile represented in figure 7.6. The triangles in the figure represent the region where the y component corresponds to the full intragrain critical current density (J_c^{grain}) and the rhombus area represents the area where the y component corresponds to the intergrain critical

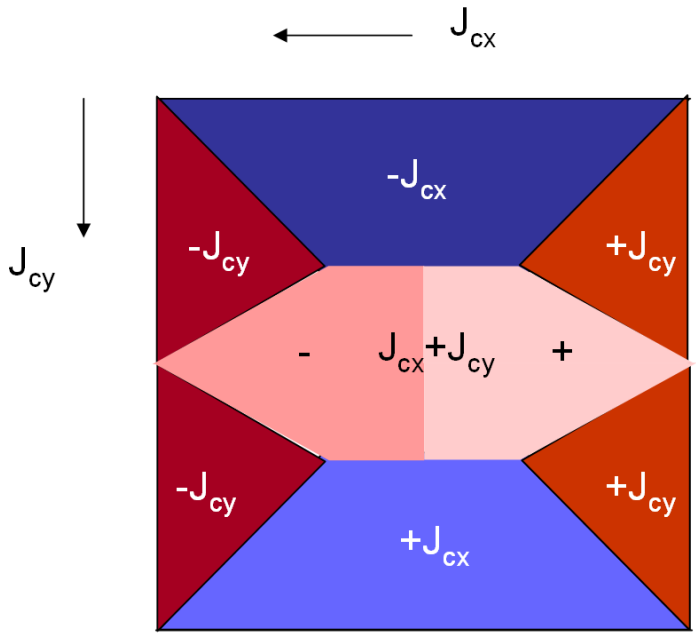

Figure 7.5: Representation of x and y component of critical current density in a bicrystal. Granatum color indicates the y component, J_{cy}, whereas blue color indicates the x component J_{cx}. The both components contribution is indicated by pink color in the figure. Dark color reflects the negative component of J_c and light color the positive component.

current density (J_c^{gb}). Thus, the value of critical current density of the grain is the value found in the triangle area and can be determined by sectioning the J_{cy} profile perpendicular to the joint and outside the rhombus area as shown in figure 7.6a. Following the Bean model, the J_{cy} is constant, forming a plateau.

The weld can be localized by sectioning the J_{cy} profile perpendicular to the junction along which, the joint and YBCO grain critical current density contributions exist (see figure 7.6b). From this profile three critical current density plateaus are obtained: two corresponding to the J_{cy} values obtained for the YBCO grains (dark granatum critical current density plateaus) and one to the J_{cy} values obtained for the junction (dark pink critical current density plateau). In the figure it is indicated that the critical current density at the dark granatum critical current density plateaus corresponding to the YBCO grains is higher than

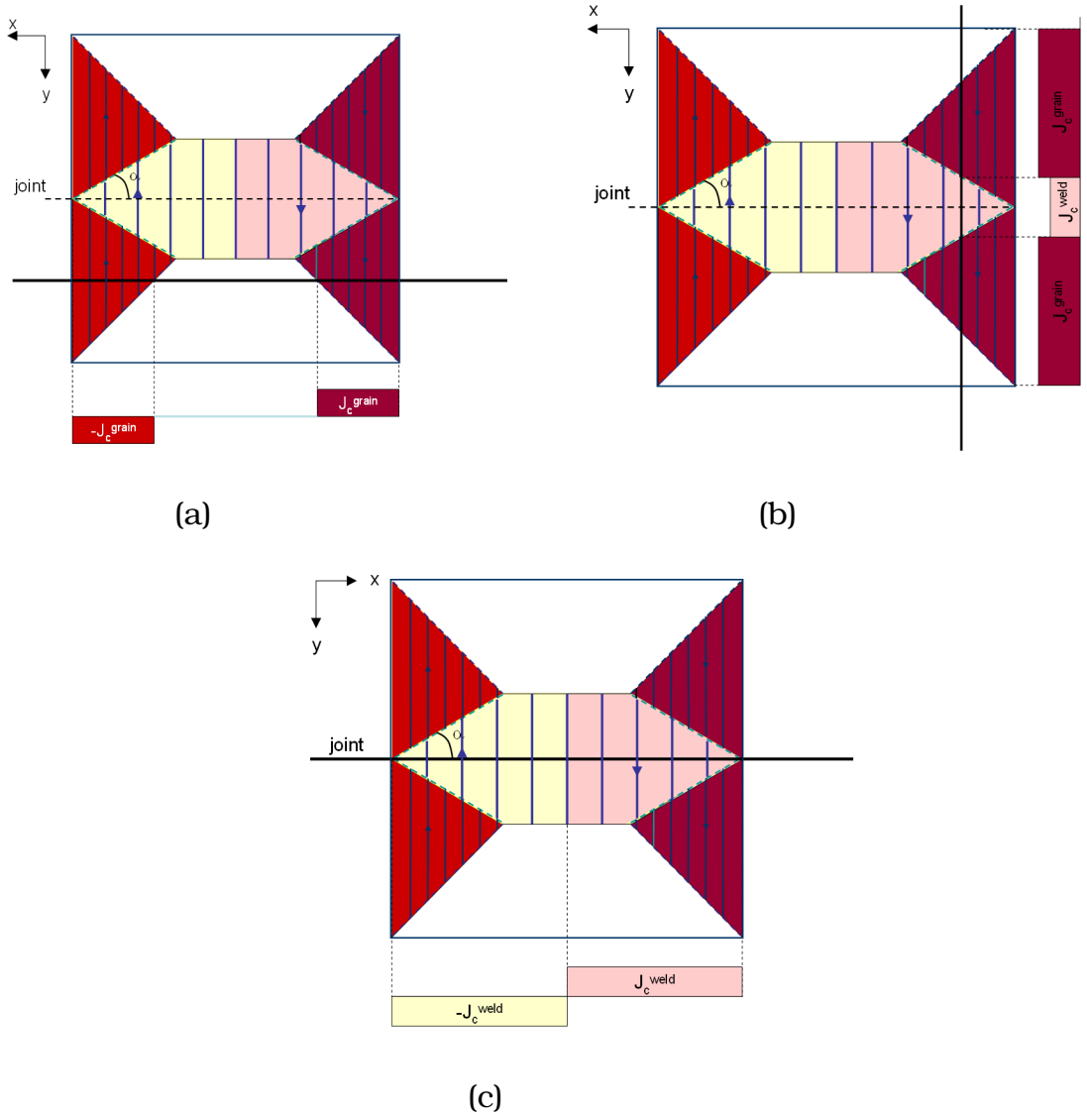

Figure 7.6: Determination of critical current density of YBCO grains and joint. a) J_{cy} of YBCO grains: section the profile parallel to the weld (outside of the rhombus area) where the y component corresponds to the full intragrain current. b) Localization of the joint: J_{cy} components profile is sectioned perpendicular to the joint along which the grain and the weld critical current contributions exist; c) J_{cy} of joint: cut the profile parallel to the weld along which J_{cy} component is associated of the current crossing the weld.

the critical current density at the dark pink critical current density plateau corresponding to the junction $J_c^{grain} > J_c^{gb}$, i.e the weld acts as a weak link for the YBCO material. In this case the angle $\alpha \neq 0$. On the other hand, if $J_c^{gb} = J_c^{grain}$, we

conclude that the quality of the joint obtained by the welding process is similar to that of the mother YBCO blocks. In this case the angle α is null, which means that the current distribution pattern should present the same profile exhibited by a single domain represented in figures 7.1(a-b). Therefore, the profile determined by sectioning the current distribution pattern perpendicular to the joint area has only one critical current density plateau corresponding to the critical current density of the sample.

Once localized the position of the joint, the J_{cy} profile is obtained along the weld line. At this line only the critical current density of the joint exists (see figure 7.6c). A positive and a negative critical current density at the current plateau corresponding to the junction can be obtained. For an homogeneous joint, the modulus of the critical current density corresponding to both current plateaus must have the same value if the Bean model is followed.

In the paragraphs to follow it will be presented the current pattern of the y component of the critical current density obtained from the magnetization measurements by employing the software "Caragol" for "real joints" after a field cooled (fc) process. First, we will present a superconducting low quality joint and second, a superconducting high quality joint, both obtained by the welding process described in Chapter 5. In figure 7.7a it is represented a 2D remanent magnetization profile obtained for a low quality joint where the junction is indicated by an arrow in the figure. As it is expected for this kind of joint, a reduction of the remanent magnetization at the junction is observed. A section of the magnetization profile perpendicular to the joint shows the presence of two peaks indicating the reduction of remanent magnetization at the joint (right side of the remanent magnetization map). Moreover, the peaks values corresponding to the YBCO grains are different, this difference being associated with some inhomogeneities in the microstructure of the starting YBCO samples or with differences in superconducting volume of both YBCO grains. Figure 7.7b shows the critical current density pattern determined from this data by using the soft-

ware "Caragol" corresponding to a low quality joint obtained after a field cooled process. It can be observed that the theoretical pattern agrees well with the experimental results. The joint is indicated by the white dashed-line. Note that the critical current density pattern exhibits four triangle areas and one rhombus area. As it was mentioned, the triangle areas correspond with zones where J_{cy} corresponds to the full intragrain critical current density. Thus, in these zones J_c^{grain} can be determined. In the rhombus area the y component, J_{cy}, corresponds to the intergrain critical current density and it is associated with the current crossing the weld. Thus, the value of J_{cy} in this area corresponds with the value of J_c^{gb}.

The first step, when a joint which acts as weak link for YBCO material is investigated, consists of determining the maximum value of J_c^{grain} through a section of the current pattern parallel to the joint and outside the rhombus area (far away from the joint) (lines joining (a) and (b), (c) and (d), respectively in figure 7.7b). In these zones only the grain contribution exists, thus the J_c^{grain} can be determined. In graphs 7.7(c-d) it can be observed that the profiles exhibit two peaks corresponding to the J_c^{grain} values at the left and at the right part of the YBCO matrix. Following the Bean model, one expects a constant critical current density J_{cy} forming a plateau as it was mentioned in figure 7.6a. However, as shown for a "real" joint, the J_{cy} plateau is not spatially constant anymore, two peaks containing a maximum and a minimum are obtained. The critical current density is strongly decreased mainly at the sample borders and the maximum value is obtained at the center of the grains. This is due mainly to the dependence of critical current density on the magnetic field. Therefore, for an homogeneous material, the four regions should exhibit the same value of the J_c^{grain}.

To determine the J_c^{gb}, a section of the critical current density pattern along the weld line is done. Note in graph (e) that profiles with two peaks are obtained. These peaks correspond to critical current density J_c values of the joint at the

right and at the left side. For an homogeneous interface, the J_c^{gb} in the right-hand side and in the left-hand side should have the same value. In practical cases, for an inhomogeneous YBCO starting material, the maximum critical current density value of the joints will be compared with the lowest value of the J_c^{grain} corresponding to the YBCO grain. This estimation is done supposing that the critical current density of the joint (J_c^{gb}) obtained by the welding process can only be lower or similar to the critical current density of the YBCO monoliths to be joined (J_c^{grain}). For instance, if the starting material is inhomogeneous, it is reasonable to expect that the critical current density of the joint should be compared with the lowest critical current density value which exhibit the YBCO grains.

A 2D remanent magnetization profile corresponding to a high quality joint is represented in figure 7.8a where the joint is indicated by an arrow. A section of the remanent magnetization profile performed perpendicular to the joint presents only a single peak as shown in the right-side of the remanent magnetization map, corresponding to the trapped flux at the center of the sample. Thus, the remanent magnetization does not decrease at the junction. In this case the whole sample acts as a unique grain which means that the current stream lines should be similar to those of a rectangle sample. The critical current density pattern of the J_{cy} determined from the software "Caragol" [96], is represented in figure 7.8b along with the theoretical current pattern which is superposed to it. A strong similarity can be observed between both patterns.

When a joint which acts as a single domain is investigated only one peak in the critical current density profile should appear. In sample shown in figure 7.8, observe that when the profile is sectioned perpendicular to the junction the peak corresponding to critical current density of Grain 1 exhibits higher value than the rest of the sample (see figure 7.8c). Observe that the critical current density profile obtained for the rest of the sample is planar which means that the junction exhibits a critical current density value similar to the critical current

density determined for the grain situated below the junction area in the figure. Thus, in the junction it cannot flow a critical current density higher than the critical current density which flows in the YBCO grain located under the junction in the figure. Additionally, observe in figure 7.8c that the profile obtained by sectioning the critical current density pattern parallel to joint in the upper part, exhibits two additional peaks corresponding to two closed critical current density loops indicated in the figure by circles. The appearance of these closed critical current density loops is mainly due to some inhomogeneities found in the YBCO starting material. Figures 7.8 (d-e) show the curves obtained by sectioning the J_{cy} profile in the upper and lower part of the joint, respectively. The maximum values obtained correspond to the critical current density values of both YBCO grains. Additionally, figure 7.8f shows the curve obtained after sectioning the profile along the joining area. The maximum values obtained correspond to the J_c^{gb}

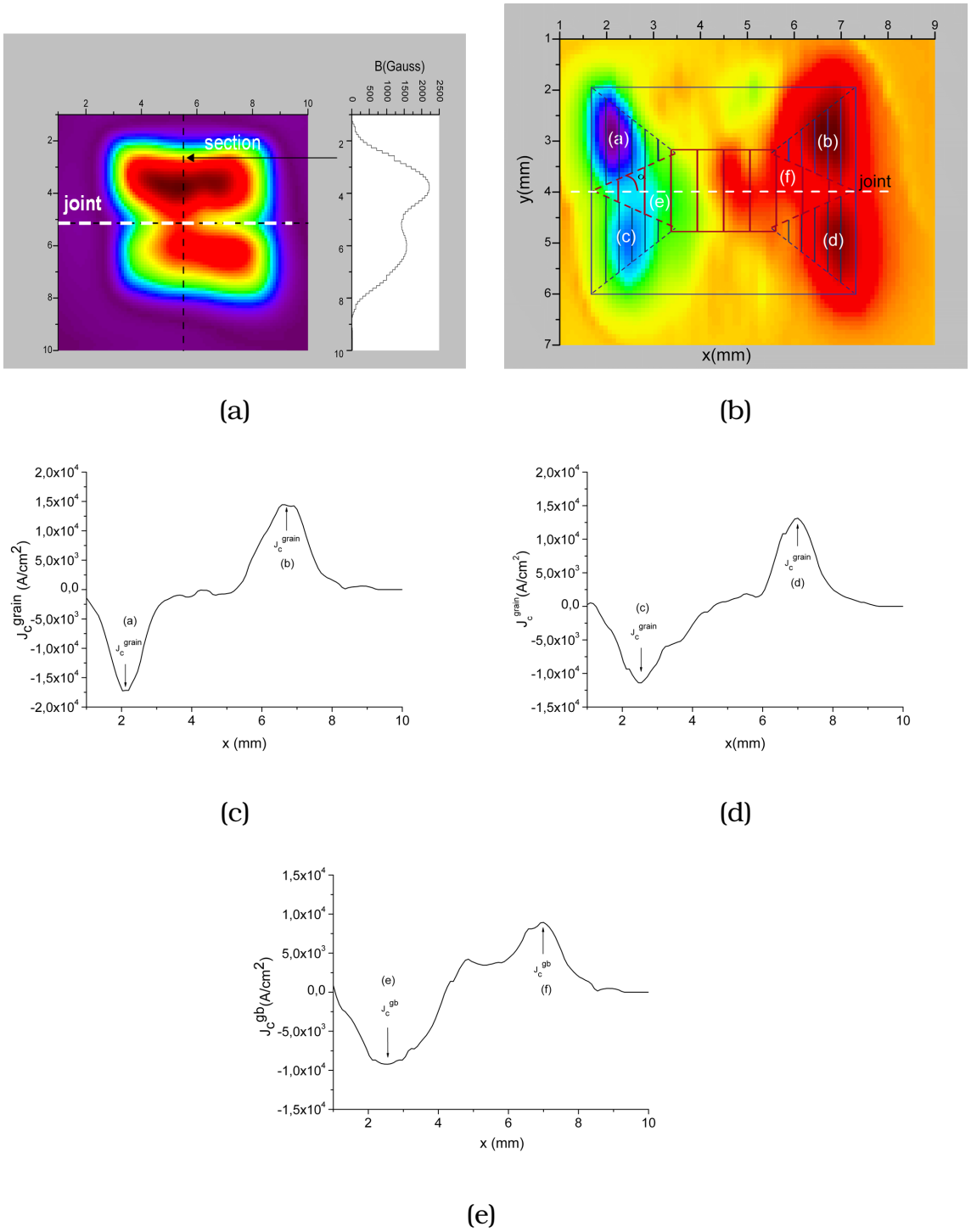

Figure 7.7: a) 2D remanent magnetization profile corresponding to a low quality superconducting "real joint". At the left side of the profile it is shown a section of this map perpendicular to the junction. The presence of two peaks can be observed. b) Critical current density pattern for the y component of the J_c obtained for a low quality "real" joint by using the Caragol software. The superposed figure corresponds with the theoretical critical current density pattern determined for the y component of J_c. The areas indicated in the figure with (a), (b), (c) and (d) correspond with the zones where the J_c^{grain} can be determined, whereas the areas (e) and (f) correspond with the zones where the J_c^{gb} is determined. c)-d) section of the critical current density pattern parallel to the joint, outside the rhombus area where only the grain contribution exists (J_c^{grain}) ((a), (b), (c) and (d)); e) section of the critical current density pattern along the joint where only the weld contribution exists (J_c^{gb}) ((e) and (f)).

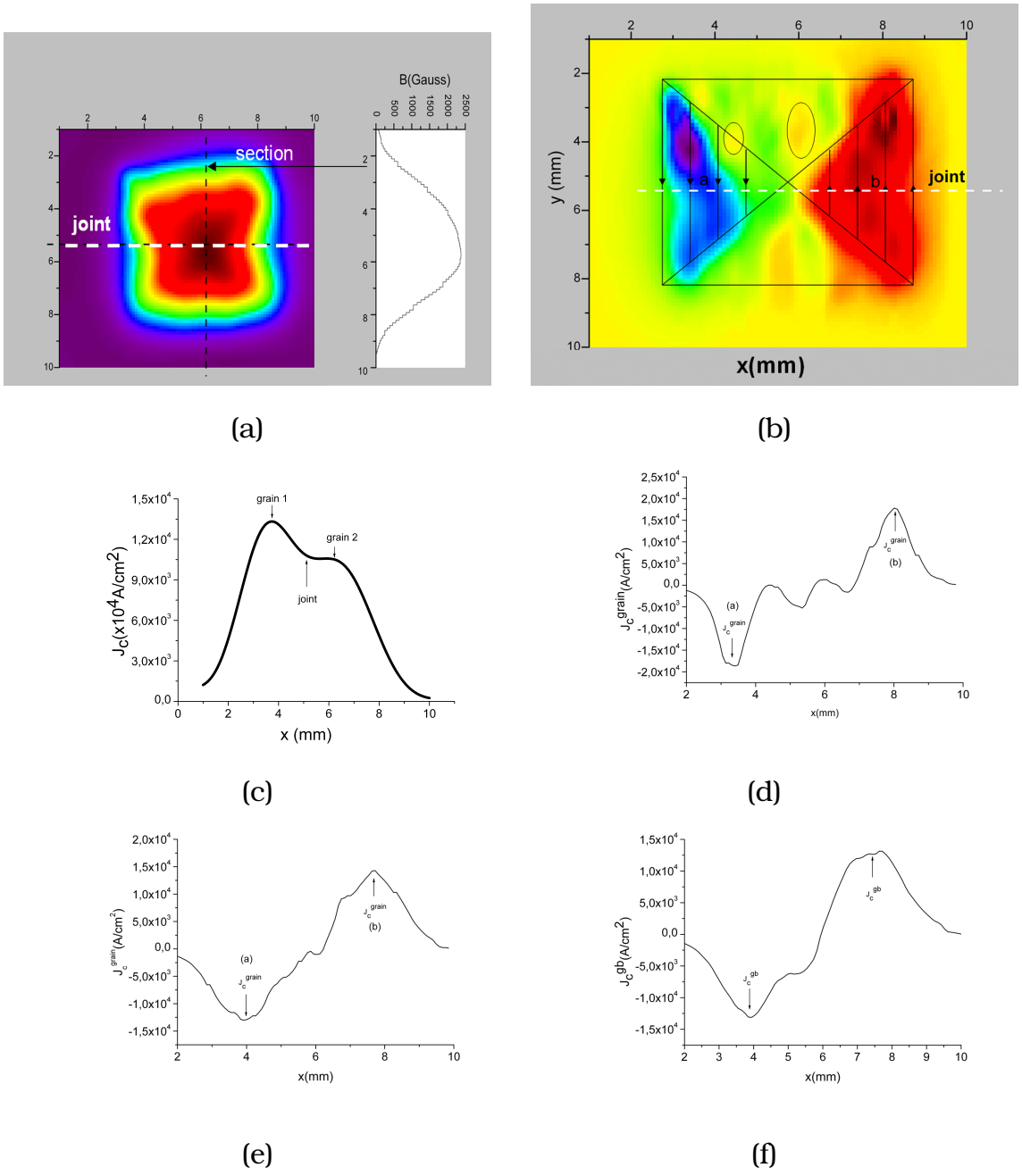

Figure 7.8: a) 2D remanent magnetization profile corresponding to a high quality superconducting "real joint". In the right side of the profile is shown a section perpendicular to the junction. The existence of only one peak corresponding to the center of the sample is shown. b) Critical current density pattern for the y component of the J_c obtained for a high quality "real" joint by using the "Caragol" software [96]. The superposed figure corresponds with the theoretical critical current density pattern determined for the y component of J_c of a single domain. The areas indicated in the figure with (a) and (b) correspond with the zones where the J_c^{grain} and J_c^{gb} can be determined as in the previous case; c) section perpendicular to the junction in region (b); d)-e) section parallel to the junction where the J^{grain} from the upper and bottom parts, respectively, are determined; f) section along the junction where only J_c^{gb} can be determined.

7.2 Detection limit of the Hall probe imaging system

In order to compare a joint with the previous YBCO single domain used for joining it is important to know the detection limit of the Hall probe imaging system and the current calculation methodology. In this way a very simple experiment has been done. We will analyze the case of a joint prepared artificially by simply gluing together two YBCO single domains. From a technological point of view these kind of samples are not interesting, but represent a very useful example from the point of view of the validation of the methodology used with the Hall system and the methodology used to determine J_c. Thus, the sample studied has a rectangular shape with a section of $0.82 \times 0.85 cm^2$ and a thickness of 0.6cm. The remanent magnetization for a single domain presents typically a single peak, corresponding to the trapping of flux at the center of the sample [69]. The decrease in the remanent magnetization along the weld, has been used before [97] as a criterion to separate bad quality joints from good ones.

In figure 7.9 it is represented a 3D remanent magnetization map corresponding to this sample after a field-cooled process. The applied magnetic field was of $H_{applied} \simeq$5000Oe and it was applied parallel to the c-axis of the sample and parallel to the joint. The junction is indicated in the figure by an arrow. It can be clearly appreciated the inhomogeneity on the remanent magnetization distribution associated with a very low superconducting quality of the junction. Moreover, observe that the left-hand side of the YBCO material displays two differentiated peaks corresponding to a reduction of the M_{rem} associated with a macrocrack (indicated in the figure). The maximum remanent magnetization measured at junction is of $M_{rem} \simeq$600 Gauss and compared with the YBCO grain is reduced by 60-70%. Thus, any joint whose remanent magnetization measured with the present Hall imaging system, is reduced by 60-70% after the welding process should be considered to be non-superconducting.

Figure 7.10 shows the calculated current distribution superposed with the remanent magnetization map after a field-cooled process. There should not be any

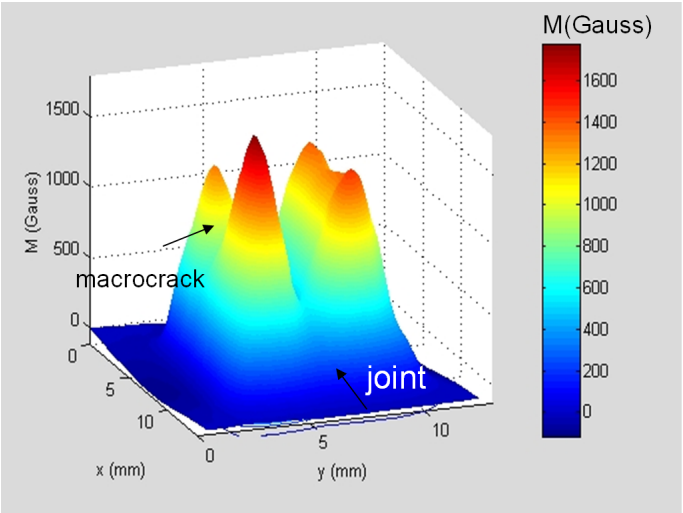

Figure 7.9: 3D remanent magnetization map for a non-superconducting joint obtained by gluing two YBCO single domains after a fc process. The joint and inhomogeneities associated with macrocraks are indicated by arrows.

connectivity between grains as it is expected for a totally non-superconducting junction. On the contrary, because of the limitations of the Hall probe imaging system there is small critical current which passes through the joint. Note that the grain situated in the upper part of the junction behaves like a single domain, the critical current density flowing homogeneously in its interior. On the contrary, the bottom grain presents two closed critical current density loops in its interior related to some inhomogeneities such macrocracks formed during the oxygenation or top seeding process.

Moreover, the critical current density of the junction is determined by employing the "Caragol" software. In figure 7.11 are represented the critical current density values calculated by using the methodology proposed by us for both grains (red and blue columns) and for the junction (yellow column). Some inhomogeneity in J_c values has been found as can be appreciated from the error bars shown in the graph. It has been found that the J_c^{grain1} is spanning between $1.42 \times 10^4 A/cm^2$ and $1.62 \times 10^4 A/cm^2$. On the contrary, J_c^{grain2} values are quite homogeneous and this grain has a critical current density of $1.4 \times 10^4 A/cm^2$. Thus,

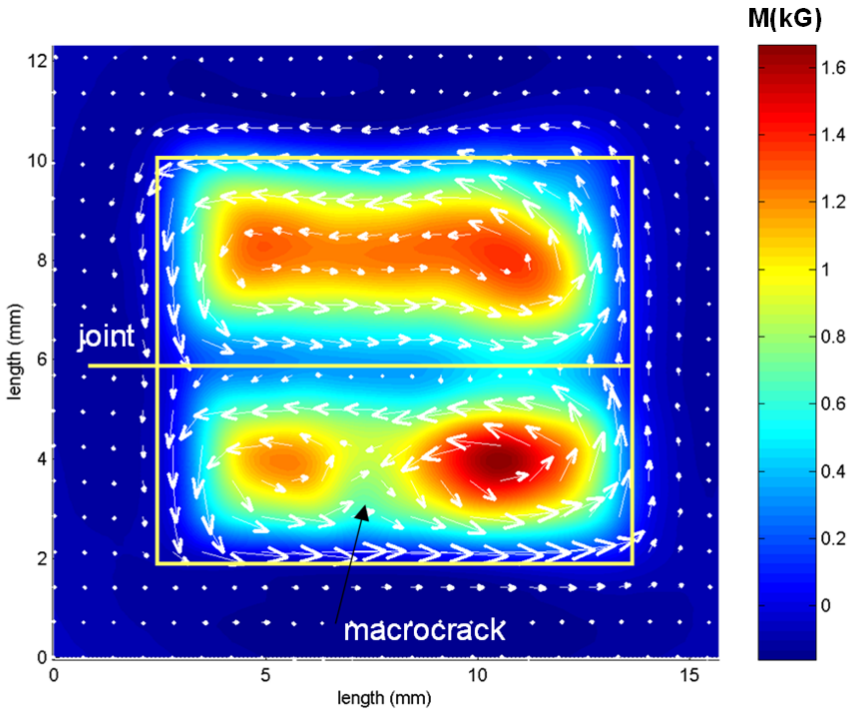

Figure 7.10: Calculated current distribution superposed with the remanent magnetization after a fc process of a sample prepared artificially by gluing two YBCO single domains. The junction is indicated in the figure and the limit of the sample are indicated for clarity.

both YBCO domains exhibit similar J_c values and the error bars indicate that some inhomogeneity exists in the proper grain. Critical current density obtained at the junction is of $5.4 \times 10^3 A/cm^2$. Thus, the ratio J_c^{gb}/J_c^{grain} is 0.38 and J_c^{gb} is reduced ≈62% from the critical current density value of the YBCO monolith if it is compared with the lowest J_c value obtained for the YBCO grain. As a consequence, any sample exhibiting J_c values across the joint that have been reduced by ≈62% after the welding process will be considered to have a poor superconducting quality and we will not be able to quantify more precisely the J_c across the joint. Moreover, according to equation 7.1 the angle α formed by d^+ lines with the junction line shown in figure 7.2, depends on the ratio J_c^{gb}/J_c^{grain}. From our results, we can discern that this ratio is 0.38 and the angle α=33°.

This means that any sample which exhibits a current pattern where the d^+ lines and grain boundary lines form an angle $\alpha \geq 33°$ is considered to be of a very low superconducting quality. One expects that for a glued sample, no current passes

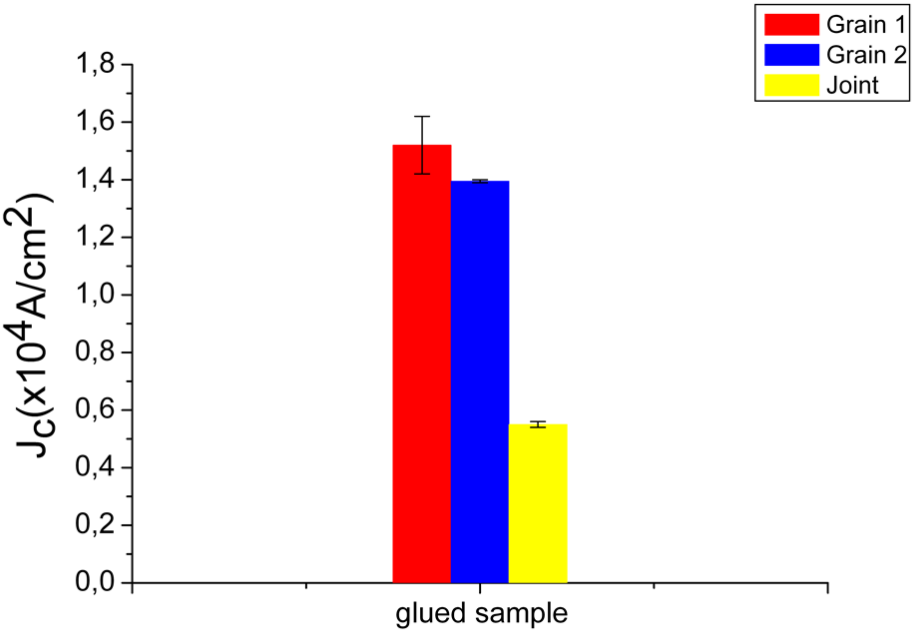

Figure 7.11: Calculated critical current density for YBCO grains and junction for a glued-sample. The red and blue columns indicate the J_c^{grain} values and the yellow column indicates the J_c^{gb} values obtained by employing the methodology described in Section 7.1. Error bars quantify the dispersion of J_c values.

through the junction and thus, the remanent magnetization and the critical current density are 0 at the junction. On the contrary, from our data we obtain that the critical current density at the junction is $5.4 \times 10^3 A/cm^2$ and that the remanent magnetization is $M_{rem} \simeq$600Gauss. The possible source of error consists in resolution of the probe, which is $0.16 \times 0.16 mm^2$, the distance between the sample and the probe which in this case is of 80μm, errors in the measurement of vertical magnetic field (error provided by the noise $\pm$ 0.2 Gauss and error coming from the resolution of the measurement which is $\sim$ 2.44 Gauss) and errors in

the numerical computation used for calculation of the critical current densities.

7.3 Optimization of oxygen content in the final joints

Since the $YBa_2Cu_3O_{7-\delta}$ type superconducting oxides were discovered, their superconductivity has been found to be sensitive to the oxygen content. Studies on high temperature oxide superconductors, indicate that oxygen concentration plays an important role in the transition temperature, magnetic properties and in achieving good pinning properties for getting higher J_c. As-grown YBCO samples are non-superconducting owing to their low oxygen content [98]. In order to obtain a high critical temperature transition and good critical current density, an oxygen loading process has to be used after the joining process. Therefore, a post-annealing in oxygen is necessary to change the structure from tetragonal to orthorhombic, which is the superconducting phase. Oxygen diffusion in YBCO depends on temperature, oxygenation time and the microstructure of the samples. Therefore, the selected time to achieve full oxygenation and oxygenation temperature will depend strongly on the size and the microstructure of the samples. Typically, for MTG samples of a few cm in size it is required to oxygenate them during several hundred hours between 350-750°C at 1 bar of O_2.

In this section we will determine a suitable time of oxygenation for the YBCO/Ag/YBCO joints studied in this work and obtained by employing the following parameters: g_{Ag}=10μm, (100)/(100) welding architecture, t_{melt}=3h, T_{max}=992°C, T_1=973°C, r=0.6°C/h and ΔT=33°C. We have observed the influence of repeated annealing steps on the remanent magnetization (M_{rem}) distribution which then, by using the "Caragol" software, is converted to the critical current density. YBCO starting samples used for joining have not been perviously oxygenated in order to avoid the formation of micro and macrocracks which could affect Ag diffusion process into YBCO matrix as it was mentioned in Chapter 6. Therefore, we did not determine the remanent magnetization and critical current densities of the previous YBCO samples for comparison. How-

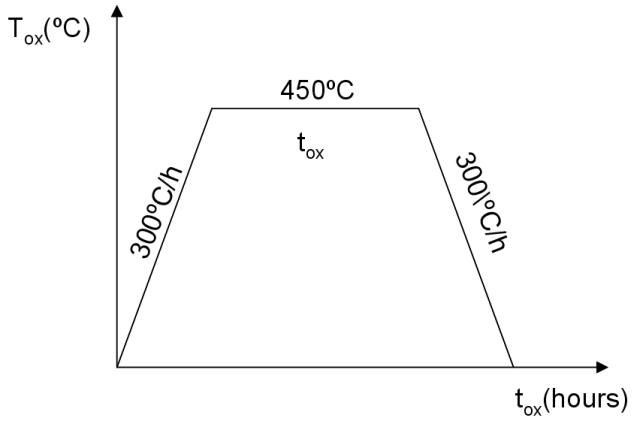

Figure 7.12: Schematic drawing illustrating the annealing cycle performed under 1 bar of oxygen flow.

ever, the methodology proposed by us to determine the critical current density of the final joints allows us to obtain simultaneously the critical current densities of both, YBCO domains and interface.

It is well-known that the oxygenation process depends on the dimensions of the sample. The joints obtained by the welding process were of rectangular shape and the dimensions are spanning between 0.86x0.94x0.6cm^3-1x1x0.6cm^3. Additionally, each YBCO grain submitted to the welding process to obtain this joint have dimensions which are slightly different: one grain has 0.42$\times$0.96$\times$0.6cm^3 whereas the other one has 0.44$\times$0.92$\times$0.6cm^3. This difference could affect the remanent magnetization at each grain. The annealing steps were performed under 1 bar of flowing oxygen. The annealing cycle consists of heating the sample to 450°C by using a rate of 200-300°C/h during several hundred hours. Then, the sample is cooled down rapidly using a 200-300°C/h rate until the ambient temperature is reached. The cycle is drawn in figure 7.12. We have used T_{ox}=450°C because it was seen in the $p_{O_2}(T)$ diagram [99] that YBCO samples have obtained optimum doping. Four different oxygenation times (t_{ox}) have been used in this study: 120, 168, 240 and 312 hours.

The remanent magnetization in the samples is studied by means of a field-

cooled process measured by using the Hall probe magnetic imaging system. Thus, the YBCO/Ag/YBCO joints are cooled down to 77K in the presence of a magnetic field of $H_{applied} \simeq$ 5000 Oe parallel to the c-axis of the sample and parallel to the joint. Once the sample reaches the liquid nitrogen temperature, the external magnetic field is removed from the sample and the scanning of the Hall probe over the ab-plane of the joint at a flying distance of 80μm in steps of 160μm is performed. In this way the remanent magnetization of the sample is determined.

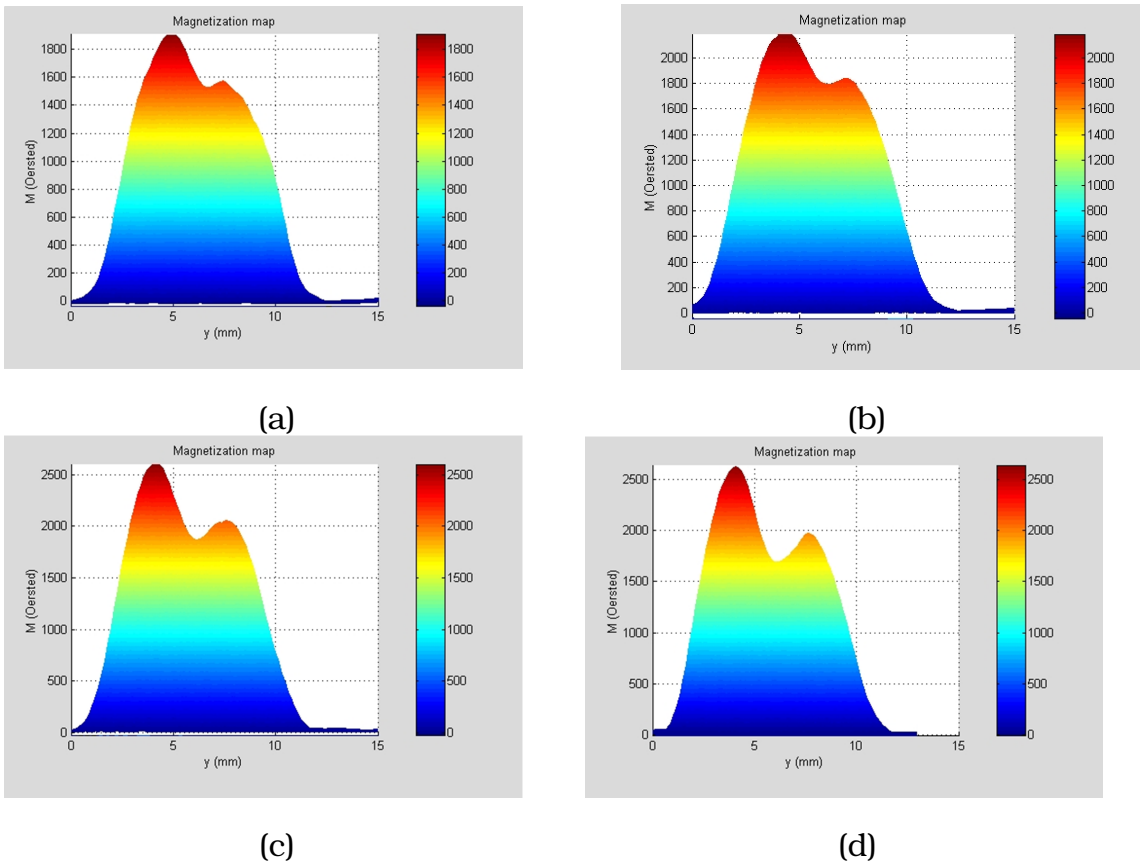

Figure 7.13: Remanent magnetization maps corresponding to different oxygenation times: a)120 hours; b)168 hours; c)240 hours and d)310 hours. In all maps we can observe two differentiated peaks showing the weak link behavior of the joint. Sample dimensions are of $\simeq$0.96x1x0.6cm^3.

Figure 7.13 (a-d) shows the remanent magnetization map after a field-cooled process when the applied field is of $\simeq$ 5000 Oe, for the four cases of oxygenation:

120, 168, 240 and 312 hours, respectively. The distribution of the remanent magnetization corresponding to the initial sample used for joining was not determined because we are using non-oxygenated MTG material. As it was mentioned in Chapter 6, when the microstructure of the samples and the influence of various parameters on it were investigated, the previous oxygenation of the samples to be joined result in the formation of micro and macrocracks which could deteriorate the superconducting quality of the joint. It has been observed (see figure 6.9 from Chapter 6), that the existence of such defects facilitates the diffusion of Ag through it which could give place to the formation of an inhomogeneous interface. Thus, the remanent magnetization is determined only on the already joined samples. It can be appreciated clearly the inhomogeneity in the distribution of remanent magnetization from the existence of a double peak profile and from the difference in the remanent magnetization values of both grains. The double peak in the profile appears because the joint acts as a weak link for the YBCO matrix, having a value of remanent magnetization lower than the rest of the sample. Moreover, the difference in the remanent magnetization of the YBCO material could be due to the existence of some inhomogeneities in the sample or to the difference in dimensions of each YBCO single domain used for the weld. It has been seen that both YBCO grains used for joining exhibited different superconducting volume. In order to see if this difference is the reason for which takes place a reduction in remanent magnetization values obtained at each grain we will treat both YBCO grain separately, as two samples. In this way we will calculate the reduction in remanent magnetization in the assumption that both YBCO grains exhibit the same critical current density when the sample is oxygenated during 168h at 450°C. The critical current density for a superconductor having parallelepiped geometry is given by equation 2.4. According to the assumption made, we will obtain that J_c^{ab}=20ΔM_1/$a_1(1-a_1/3b_1)$= 20ΔM_2/$a_2(1-a_2/3b_2)$,where a_1, b_1 and a_2, b_2 are the dimensions of transverse section, to which the magnetic field is perpendicular with the condition that a<b. In this case we obtain that

the reduction in remanent magnetization taking into account this assumption is of ∼3%. To determine this ratio M_1/M_2 from the experimental data we should ensure the separation of remanent magnetization at the joint area from the remanent magnetization contribution of YBCO grains. This separation has been ensured by fitting the remanent magnetization profile according to the gaussian equation 7.2.

$$y = y_0 + \frac{A}{w\sqrt{\pi/2}} e^{-2\frac{(x-x_c)^2}{w^2}} \tag{7.2}$$

where A is the area, w is the width, y_0 is the offset and x_c is the center of the peak.

Figure 7.14 shows the experimental remanent magnetization profile obtained for the joint (red line in the figure), the contribution of both YBCO grains (blue lines) and the gaussian fit of the experimental profile (yellow line). The fitted profile is adjusted quite well to the experimental profile. After the separation of the remanent magnetization contribution of the joint from the remanent magnetization contribution of the YBCO grains we obtain that the reduction in remanent magnetization is 19% which is higher than the value calculated by using the formula of J_c for a parallelepiped geometry. Thus, the reduction in remanent magnetization can be attributed to an inhomogeneity between the two YBCO grains, i.e. they display different J_c.

An overview of the remanent magnetization dependence with the annealing time in oxygen atmosphere for the YBCO/Ag/YBCO joint is represented in figure 7.15. The yellow symbols correspond to the joint, the red symbols to the Grain 1 and the blue symbols to the Grain 2. It is interesting to observe that by increasing the oxygenation time up to a certain value, the remanent magnetization of both grains and joint is increasing. Unfortunately, this value of oxygenation time is not the same for the joint and for the grains. Note that the remanent magnetization of the joint achieves a maximum faster than the YBCO grains. When the oxygenation time was of t_{ox}=168h, the joint is already in the optimum state.

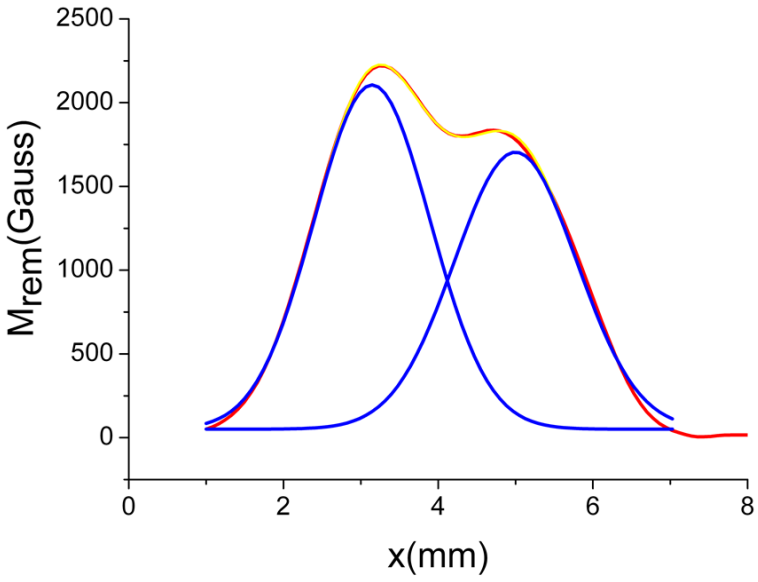

Figure 7.14: Red line: Section of the remanent magnetization profile obtained for the sample. Blue lines: Remanent magnetization profile obtained for each YBCO grain after the fitting of experimental data. Yellow line: Gaussian fit of the experimental remanent magnetization profile. The sample studied is oxygenated for 168h at 450°C.

With further increasing of the oxygenation time, the remanent magnetization at the joint is kept constant. The optimum state is achieved by both grains when t_{ox}=240h. As in the previous case, with further increasing of the oxygenation time, the remanent magnetization is constant. For a joint which acts as weak link for the YBCO material, there are two types of diffusion during the oxygenation process: oxygen diffusion along the grain boundary and oxygen diffusion through the well-connected YBCO grains. According to these results, the optimum state is achieved faster by the joint because of its weak link behavior, the oxygen diffusion through the joint being faster than through the grain.

In figure 7.16 it is represented the critical current density (J_c) dependence with the annealing time for both YBCO grains (red and blue symbols) and final joint (yellow symbols). The error bars in the figure quantify the dispersion on the

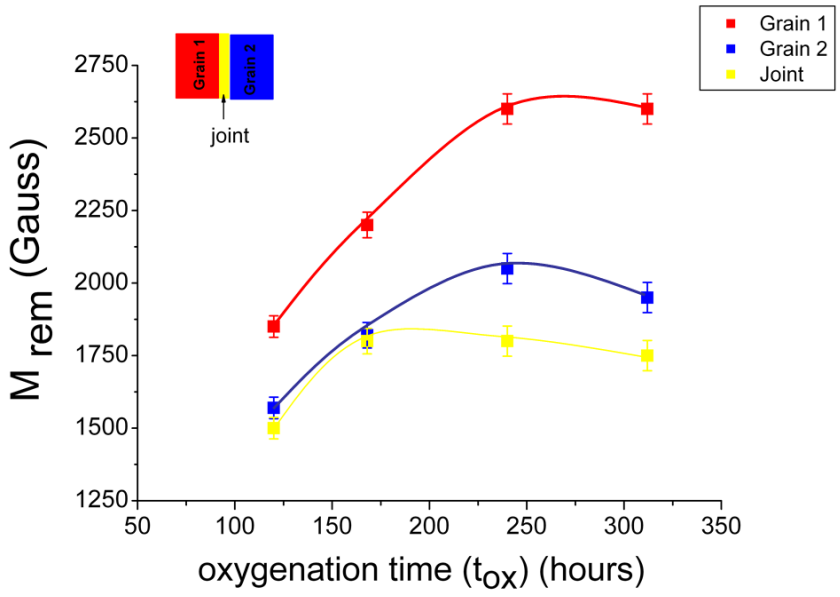

Figure 7.15: Remanent magnetization of the YBCO/Ag/YBCO joints versus the annealing time under 1 bar oxygen at 450°C. The Grain 1 and Grain 2 are represented by the red and blue symbols respectively. The joint is represented by the yellow symbols., A schematic representation of the configuration of the grains and joint is presented in the inset of the figure.

J_c values calculated by using the methodology described in Section 7.1 for each annealing step. These error bars indicate that the YBCO grains used for joining are slightly inhomogeneous and that each YBCO grain exhibits itself some inhomogeneity which result in the existence of a large dispersion of J_c values within each grain. According to the results presented in figure 7.16, the critical current density of both grains is increasing with increasing the oxygenation time up to t_{ox}=240h. Then, with further increasing of t_{ox}, the J_c^{grain} is maintained constant. For t_{ox}=240h, the $J_c^{grain1} \simeq 1.8 \times 10^4 A/cm^2$ and $J_c^{grain2} \simeq 1.55 \times 10^4 A/cm^2$. On the contrary, when the joint is investigated, it can be observed that the critical current density reaches its maximum value for t_{ox}=168h. With further increasing of t_{ox} the J_c^{gb} is maintained constant ($J_c^{gb} \simeq 0.89 \times 10^4 A/cm^2$).

For comparison purposes, in figure 7.17 it is represented the dependence

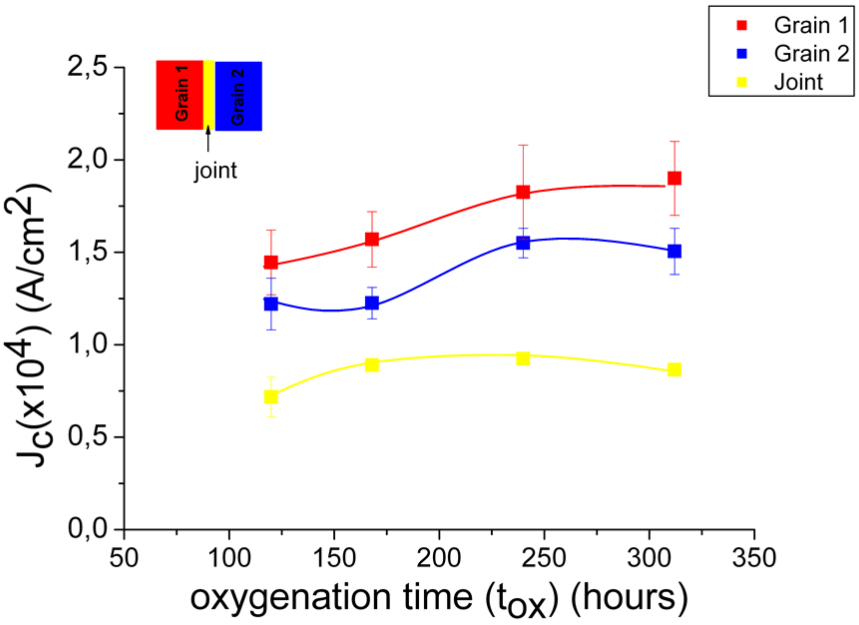

Figure 7.16: Critical current density of the YBCO/Ag/YBCO joints as a function of the annealing time in oxygen atmosphere. The red and blue lines correspond to the YBCO grains and the yellow line to the joint. The error bars quantify the dispersion on J_c values for both YBCO grain and joint.

with the oxygenation time of the ratio J_c^{gb}/J_c^{grain}, where J_c^{grain} represents the critical current density corresponding to the lower value exhibited by YBCO grains. This ratio shows the percentage of the reduction of the critical current density of joint (J_c^{gb}) after the welding process when compared with the lowest value of critical current density obtained for YBCO grains. The error bars in the figure quantify the dispersion on J_c^{gb}/J_c^{grain} values calculated by using the methodology described in Section 7.1 for each case. It can be observed that if t_{ox}=168h, when the joint is in the optimum state, the J_c^{gb} is reduced by 27% from the J_c^{grain}. But it is important to remember that at this time t_{ox}=168h, the YBCO grains did not achieve the optimum state. Thus, when both grains have achieved this state, at t_{ox}=240h, the critical current density of the joint J_c^{gb} is reduced by 40% from the

J_c^{grain}.

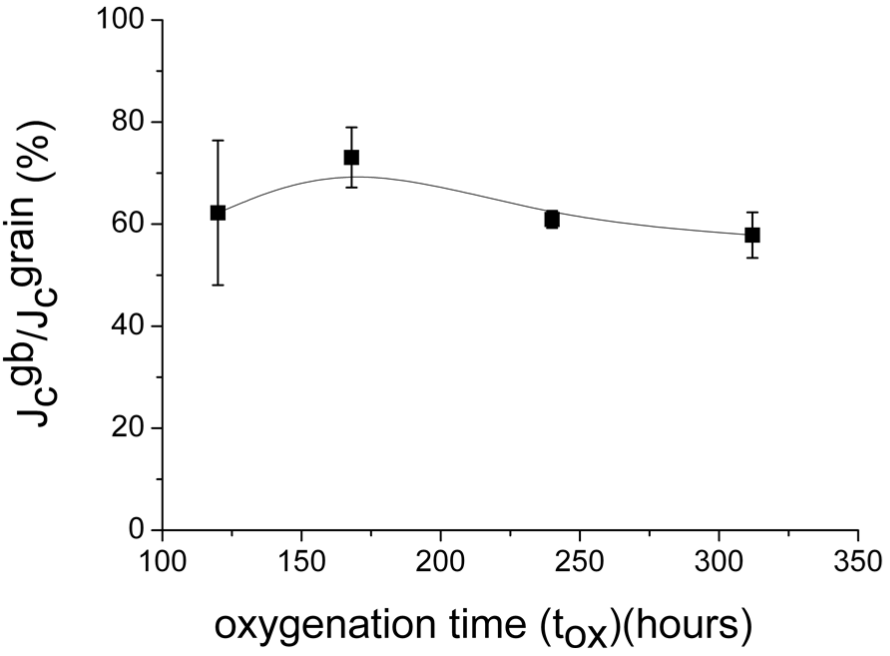

Figure 7.17: Dependence of the ratio J_c^{gb}/J_c^{grain} with the oxygenation time. The J_c^{gb} represents the critical current density of the joint and J_c^{grain} represents the lowest critical current density value exhibited by the YBCO grains. This ratio gives us the percentage of the reduction of the J_c^{gb} after the welding process. The error bars in the figure quantify the dispersion of J_c^{gb}/J_c^{grain} values.

According to our results, the oxygen diffusion through the investigated joint is slightly faster than the oxygen diffusion through the YBCO grain since the joint needed a smaller oxygenation time to achieve the optimum state. Thus, we decided that the optimum oxygenation time for joints obtained by using this welding process and with the sample sizes used in this work is between 168h and 240h. Further investigation of other parameters which could affect the quality of the superconducting joints has been performed in samples annealed in 1 bar oxygen atmosphere for 168 hours to 240 hours at 450°C.